Prevalence and mechanisms of high-level carbapenem antibiotic tolerance in clinical isolates of *Klebsiella pneumoniae*

Authors: Trevor Cross[1,2], Facundo Torres[1,2], Abigail P. McGee[2*], Tolani Aliyu[2], Lars F. Westblade[3], Abhyudai Singh[4], Tobias Dörr[1,2,5]

[1]Department of Microbiology, Cornell University, Ithaca, NY

[2]Weill Institute for Cell and Molecular Biology, Cornell University, Ithaca, NY

[3] Departments of Pathology and Laboratory Medicine, Medicine, and Pediatrics, Weill Cornell Medicine, New York, NY

[4] Department of Electrical and Computer Engineering, University of Delaware, Newark, DE, 19716, USA

[5] Cornell Institute for Host-Microbe Interactions and Disease (CIHMID)

[*]Current affiliation: Graduate Program in Microbiology and Immunology, Geisel School of Medicine, Dartmouth

Keywords: meropenem, cell envelope stress response, spheroplast, L-form, MltB

Abstract:

Antibiotic tolerance is the ability of bacteria to survive normally lethal doses of antibiotics for extended time periods. Clinically significant Enterobacterales, for example, often exhibit high tolerance to the last-resort antibiotic meropenem. Meropenem tolerance is associated with formation of cell wall-deficient spheroplasts that readily recover to rod shape and normal growth upon removal of the antibiotic. Both the true prevalence of tolerance, and genetic mechanisms underlying it, remain poorly understood. Here, we find that meropenem tolerance is widespread among clinical Enterobacterales. Using forward genetics, we uncover novel tolerance factors in a hypertolerant isolate of the

ESKAPE pathogen *Klebsiella pneumoniae*. We find that multiple mechanisms contribute to tolerance, and that cell envelope stress responses (PhoPQ, Cpx, Rcs and OmpR/EnvZ) collectively promote spheroplast stability and recovery, while the lytic transglycosylase MltB counteracts it. Our data indicate that tolerance is widespread among clinical isolates, and that outer membrane maintenance is a key factor promoting survival of tolerant *K. pneumoniae.*

Introduction

Healthcare-associated infections are common sequelae of hospitalization and increasingly, treatment of these infections fails due to antibiotic resistance [1]. However, treatment also often fails despite the absence of outright resistance [2]. This has been attributed to other strategies bacteria have for evading complete eradication, including the well-characterized phenomenon of bacterial persistence [3]. However, between the extremes of frank resistance and persistence there is considerable complexity in bacterial antibiotic susceptibility patterns. For example, antibiotic tolerance, which has recently received increased attention as another means of surviving antibiotic insult, represents a state where a large fraction of a susceptible bacterial population survives in the presence of an antibiotic for extended periods. Gram-negative bacteria in particular can enter a non-replicative, cell wall-deficient spheroplast form upon treatment with β-lactam antibiotics [4-7]. This phenotype is reminiscent of L-forms [8-10] with the distinction that spheroplasts (unlike L-forms) do not proliferate in the presence of antibiotic. Spheroplasts remain intact for extended time periods and readily recover their cell shape and resume

division when the β-lactam drug is removed. However, the true prevalence of β-lactam tolerant Gram-negative pathogens among clinical isolates is unknown.

Klebsiella pneumoniae is a Gram-negative nosocomial pathogen that can cause a variety of opportunistic infections, including eponymous pneumonia, bloodstream infections and UTIs [11]. A member of the infamous ESKAPE group of pathogens, *K. pneumoniae* exhibits particularly worrisome levels of treatment failure [12]. Due to the high level of resistance against most β-lactams, the carbapenems remain one of the leading antibiotic classes that are effective against *K. pneumoniae* [13]. Determining mechanisms that alter susceptibility against β-lactams in general, and carbapenems in particular, is thus a critical need for developing new treatment options against *K. pneumoniae.*

β-lactams covalently and irreversibly bind to so-called penicillin-binding proteins (PBPs), which are the principal synthases of the main cell wall component peptidoglycan (PG). β-lactam binding results in several downstream events that contribute to cell death in poorly-defined ways [14]. Endogenous cell wall lytic enzymes (collectively referred to as autolysins) degrade the PG sacculus into monomers and ultimately eliminate the sacculus entirely. In some bacteria, cell wall degradation can cause catastrophic rupture and cell lysis, for example in the well-studied model organism *E. coli.* In addition, the constant synthesis and immediate autolysin-mediated degradation of PG (futile cycling) depletes cellular resources, exacerbating detrimental effects independent of cell lysis [15, 16]. Interestingly, β-lactam exposure coincides with the generation of damaging reactive oxygen species (ROS), though the contribution of ROS to β-lactam killing is not entirely clear [17]. It is thought that the combination of these direct and indirect effects likely

collectively contributes to cell death by lysis or internal damage. How tolerant cells manage this assault to stay alive has remained poorly understood, but previous work has implicated cell envelope stress signaling in spheroplast survival [17-19]. In the cholera pathogen *Vibrio cholerae*, for example, the VxrAB system is induced by β-lactam stress, resulting in the upregulation of cell wall synthesis functions (which readies the cell for recovery once the antibiotic is removed) and downregulation of detrimental iron influx (putatively to reduce the damage sustained by ROS production) [17].

In this study, we sought to characterize meropenem tolerance in *K. pneumoniae*. We found that clinical isolates of this nosocomial Gram-negative pathogen often exhibit high levels of meropenem tolerance. Using TnSeq, we defined genetic requirements for tolerance, and uncovered a role for cell envelope stress signaling systems in both spheroplast maintenance and recovery. Our data open the door for a more in-depth understanding of the molecular mechanisms promoting tolerance, priming the future design of antibiotic adjuvants that eradicate tolerant cells.

Results

Klebsiella species clinical isolates exhibit high meropenem tolerance

As part of a larger effort to determine the role of antibiotic tolerance in healthcare settings, we characterized a large panel of bloodstream isolates from the culture collection of Weill Cornell Medical (WCM). This de-identified 271 isolate panel (Table S1) is fully characterized through antimicrobial susceptibility testing and consists of a large number

91 of mostly carbapenem-susceptible (MIC <1 μg/mL) Gram-negative pathogens, with three
92 isolates testing as intermediate (MIC = 2) and seven strains as fully resistant (MIC > 4
93 μg/mL; one strain due to its possession of the KPC carbapenemase). Since the majority
94 of the isolates are carbapenem susceptible, we considered this an ideal panel for
95 determination of how prevalent carbapenem tolerance (rather than resistance) is in
96 clinical samples. Currently, no fully-established sufficiently high throughput tolerance
97 assay exists [20], and we therefore chose to use a semi-quantitative assay for our screen.
98 To this end, we grew the isolate panel (curated to remove the resistant isolates with MIC
99 > 4 μg/mL) in a 96-well format, where we exposed cells to meropenem (10 μg/mL, 5x –
100 100x MIC) at high cell densities (following a 10-fold dilution of overnight culture into fresh
101 medium). At an eight-hour timepoint, 5 μL of thus-treated cultures were then spotted on
102 an agar plate together with 5 ng of purified carbapenemase (KPC-2) to remove the
103 antibiotic. After 24 hours of incubation, spots were then scored as full growth (a confluent
104 spot = high tolerance), growth with a few visible colonies (= intermediate) or no growth (=
105 low tolerance) (**Fig. 1A, S1**). Since this panel contained isolates exhibiting a wide
106 distribution of susceptibilities to meropenem (MICs ranging from ≤0.015 – 4 μg/mL), we
107 considered the possibility that apparent differences in tolerance may instead indicate
108 differences in MIC. Plotting tolerance categories over MIC values revealed that all 3
109 tolerance categories contained isolates with similar variance in MICs (**Fig. 1B**). As an
110 example, all isolates in **Fig. 1A** with a yellow circle had comparatively high MICs (>1
111 μg/mL), but displayed very different survival levels at 8 and 24 hours of meropenem
112 exposure. Thus, tolerance as determined in this assay is not a simple function of MIC
113 variation; rather, these data suggest that our assay captures true tolerance.

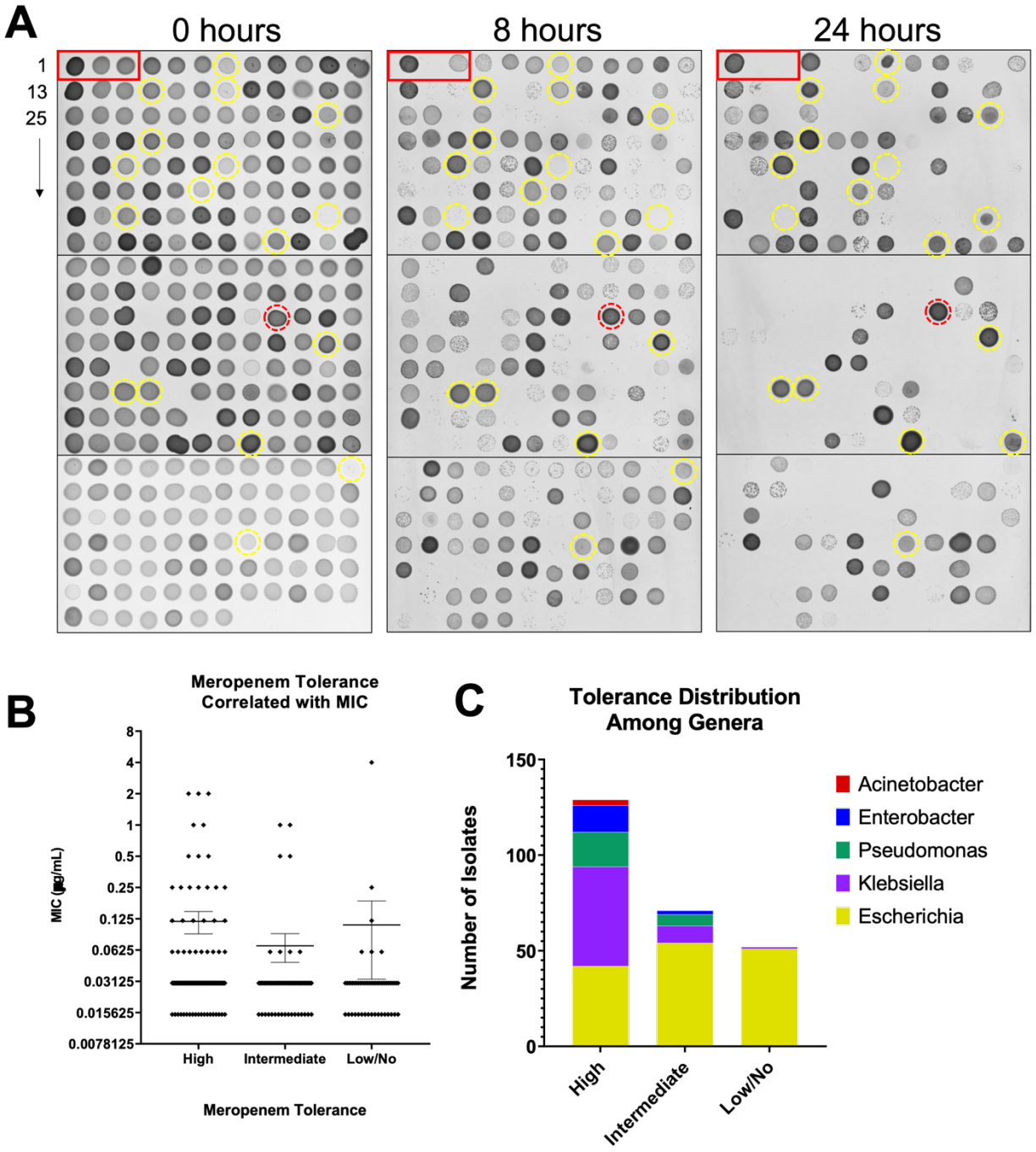

Figure 1: Widespread meropenem tolerance among bloodstream isolates

(A) A panel of bloodstream isolates was exposed to 10 µg/mL (>2x MIC for all isolates) meropenem in 96-well format (BHI medium) and incubated for 8 hours or 24 hours. Following incubation, purified KPC-2 enzyme was added to the wells, and 10 µL transferred to a BHI plate without antibiotic. Tolerance was scored qualitatively as the ability to form colonies/confluent growth after 8 or 24 hours. Yellow circles indicate examples of different tolerance levels across high MIC (>/=1 µg/mL). Red circle indicates

122 the positive control (resistant KPC+ strain). Red box indicates examples of (from left to
123 right) a highly tolerant *Klebsiella pneumoniae* isolate, a medium tolerant *E. coli* and a low
124 tolerance *E. coli.* (B) Tolerance categories were plotted with their corresponding MIC
125 values. (C) Genus distribution among the tolerance categories.

126

127 We then asked whether some genera were more likely to display tolerance than
128 others, and to this end plotted tolerance as a function of bacterial genus. Interestingly, the
129 low tolerance fraction was almost exclusively occupied by *E. coli* isolates (consistent with
130 our previous observations [7]), while the high tolerance fraction was enriched in
131 *Enterobacter species., Pseudomonas aeruginosa*, and especially *Klebsiella pneumoniae*
132 (**Fig. 1C**). Thus, *K. pneumoniae* clinical isolates are particularly likely to display antibiotic
133 tolerance among clinical isolates of Enterobacterales.

134

135 *The K. pneumoniae TS1 isolate is highly meropenem tolerant*

136 Since *K. pneumoniae* clinical isolates answered our survey as particularly tolerant,
137 we chose to focus on this species for further study of meropenem tolerance. However,
138 we noted that different *K. pneumoniae* isolates diverged in tolerance levels in our spot
139 assay (**Fig. 1A**). To more quantitatively determine strain-specific differences, and to
140 identify new model strains for mechanistic studies, we compared two well-characterized
141 clinical isolates of *K. pneumoniae* for their tolerance levels *in vitro*, namely *K. pneumoniae*
142 strains TS1 (a derivative of the CDC isolate bank AR0080) and KPNIH1 [21]. Both strains
143 have been cured of their carbapenemase-containing plasmids and are thus fully
144 meropenem susceptible (**Table S2** MICs). Time-dependent killing experiments in the

145 presence of 10 µg/mL meropenem revealed drastic differences in tolerance levels

146 between the two strains, despite their similarly low MICs (**Fig. 2, Table S2**).

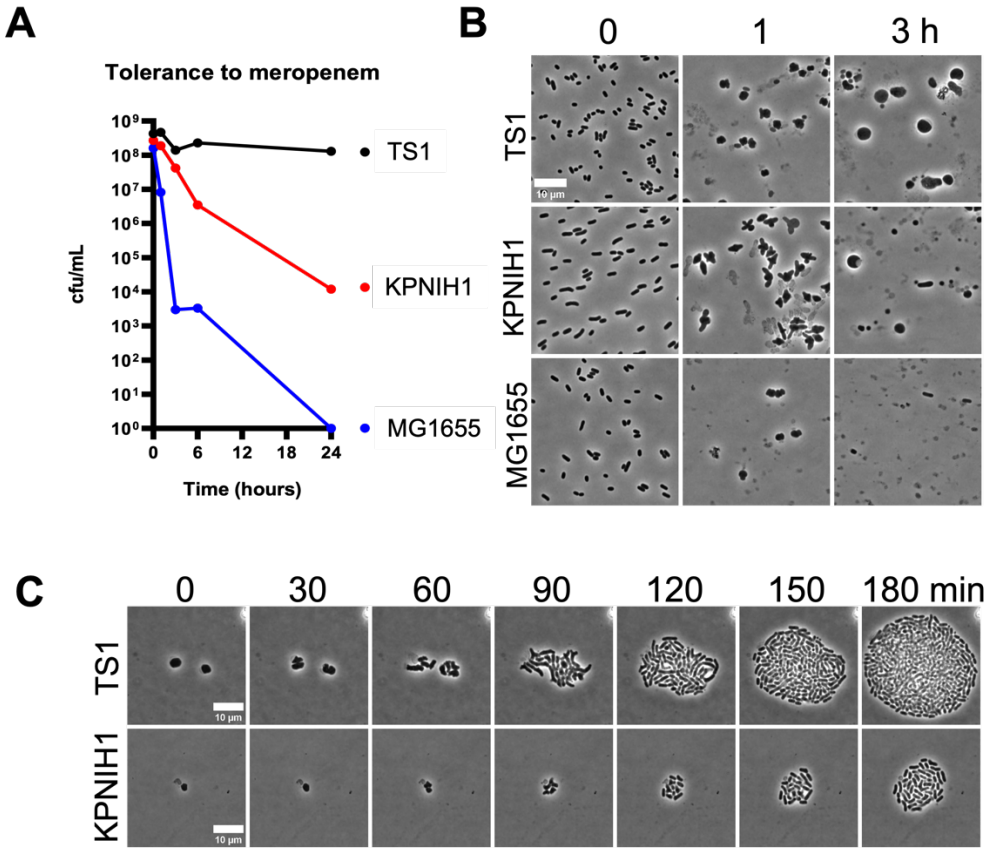

147

148 **Figure 2: *K. pneumoniae* TS1 is a hypertolerant clinical isolate**

149 (A) Example time-dependent killing experiment (BHI medium) in meropenem (10 µg/mL)
150 reveals differences in tolerance levels among two *K. pneumoniae* isolates (with the model
151 *E. coli* strain MG1655 as comparison). (B) Tolerance in *K. pneumoniae* is associated with
152 spheroplast formation. Aliquots from the experiment depicted in panel (A) were
153 transferred to agarose slides at the indicated time-points and imaged. (C) Recovery after
154 addition of purified KPC-2 carbapenemase demonstrates spheroplast viability.

155

156 This observation supports our previous finding of widely different tolerance levels

157 between different isolates of the same species [7]. Both *K. pneumoniae* strains still

158 exhibited higher levels of survival relative to the low-tolerance *E. coli* MG1655 comparison

159 strain, which exhibited a steep, 4.5 log reduction in viability within six hours of meropenem
160 treatment, and complete elimination by 24 hours of exposure. The TS1 strain was almost
161 completely tolerant, with only a slight (5-10 fold) decrease in viability even after 24 hours
162 of exposure (**Fig. 2A**). In contrast, the KPNIH1 isolate drastically lost viability by 10,000-
163 fold after 24 hours. In *both Klebsiella* isolates, survival coincided with formation of cell
164 wall-deficient spheroplasts (**Fig. 2B**) that readily recovered to rod-shape morphology
165 upon removal of the antibiotic (**Fig. 2C**). We also used these three benchmark strains to
166 validate our high-tolerance spot assay (**Fig. 1A**). Consistent with the time-dependent
167 killing experiments (**Fig. 2A**), TS1 scored as highly tolerant, KPNIH1 as intermediate, and
168 MG1655 as non-tolerant in the spot assay (**Fig. S1**). Thus, the TS1 isolate is highly
169 meropenem tolerant, and serves as an ideal model for a mechanistic characterization of
170 spheroplast formation and recovery.

171

172 *A TnSeq approach reveals putative tolerance genes in K. pneumoniae* TS1

173 We next sought to identify factors that contribute to meropenem tolerance in *K.*
174 *pneumoniae*. To this end, we conducted a transposon-insertion sequencing screen to
175 assemble a genome-wide mutant fitness map in the presence of meropenem and
176 compared insertion frequencies before and after 6 hours of meropenem challenge
177 (including an outgrowth step, see methods for details, **Fig. 3A**).

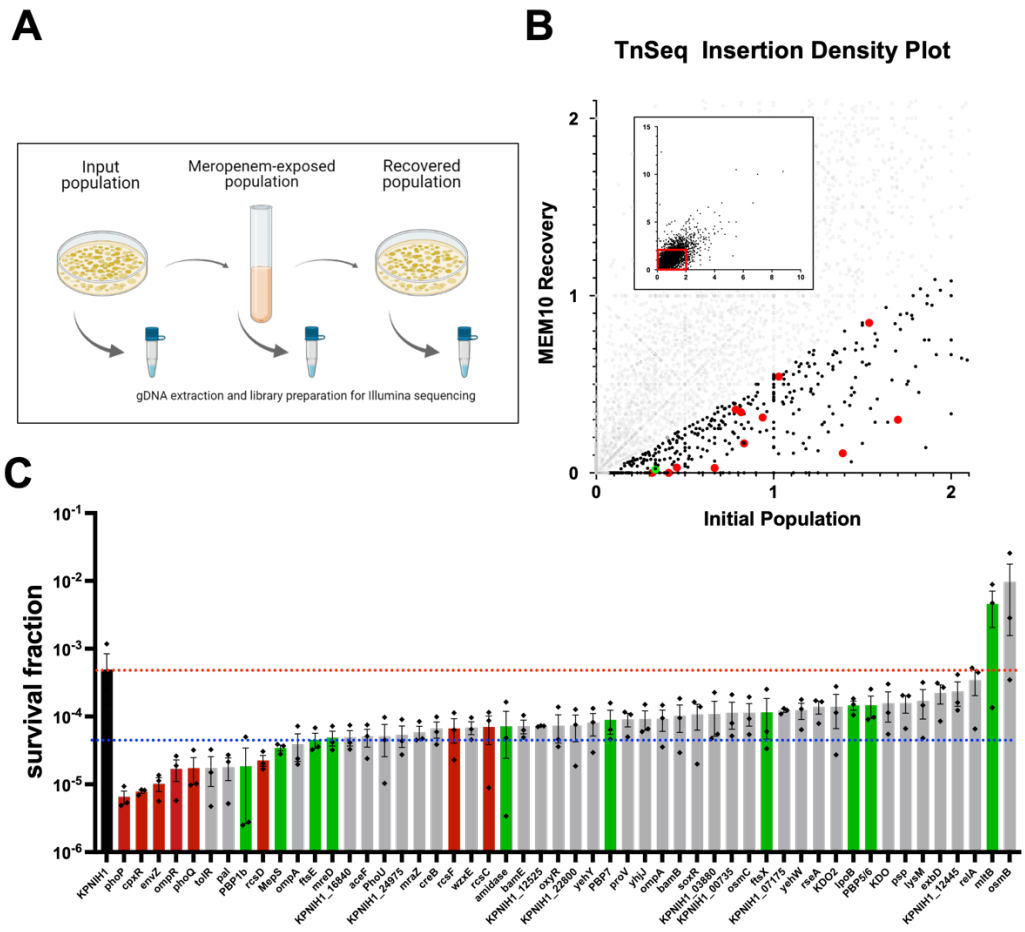

Figure 3: TnSeq identifies genetic determinants of meropenem tolerance.

(A) Outline of TnSeq experimental procedure. (B) Identification of significant candidate tolerance factors in TS1 by plotting insertion density of a recovered library vs. the input library. (C) Validation of TnSeq hits. Mutants were obtained from the KPNIH1 mutant library and exposed to meropenem (10 µg/mL) for 6 hours, followed by dilution and spot-plating. Raw data of 3 independent biological replicates are shown +/- standard deviation. Red dotted line indicates WT average survival level; blue dotted line represents the 10fold reduced survival benchmark.

The screen uncovered many expected and novel putative tolerance genes (**Fig. 3B**). Notably, the gene coding for PBP1b was detected within the top two percent of candidate essential genes for tolerance to meropenem. Class aPBPs like aPBP1b have an established role in rebuilding the cell wall after damage [22, 23], and thus serve as

192 internal validation of our screening conditions, establishing confidence in our screening
193 approach. Next, we validated our most prominent (top 10%) hits. We used an ordered,
194 commercially available transposon insertion library in the intermediate tolerance strain
195 KPNIH1 [21] for a first-pass validation. This resulted in confirmation of several genes
196 whose inactivation either promoted or decreased tolerance (**Fig. 3C**). The reduced
197 tolerance fraction was enriched in cell envelope functions (**Fig. 3C**, green bars), which is
198 expected due to the need to re-establish a cell wall upon spheroplast recovery. We also
199 noticed that disruptions in several cell envelope stress response systems (*rcs*, *pho*, *cpx*,
200 and *ompR-envZ*), drastically reduced survival during meropenem stress (**Fig. 3C**, red
201 bars), while two gene disruptions (in the gene for the cell wall lytic enzyme MltB, and in
202 the poorly characterized outer membrane lipoprotein OsmB), increased survival. Taken
203 together, these results demonstrate that the *K. pneumoniae* TnSeq experiment was
204 effective at identifying specific genes with roles in meropenem tolerance, lending
205 themselves to further study as outlined below.

206

207 *The lytic transglycosylase* MltB *endogenously reduces meropenem tolerance*

208 Our TnSeq screen identified both genes that promote meropenem tolerance as
209 well as genes which endogenously reduce tolerance. The gene coding for the lytic
210 transglycosylase enzyme MltB, for example, answered the screen as imparting a severe
211 fitness cost in the presence of meropenem. This was unexpected, since bacteria have
212 many functionally redundant lytic transglycosylase paralogs throughout their genomes,
213 and phenotypes associated with a single deletion are thus rare [24]. To dissect the role
214 of LTGs in meropenem tolerance further, we tested a panel of transposon disruption

mutants in known and predicted LTG genes for meropenem tolerance in the lower tolerance strain KPNIH1. Among eleven mutants tested, only *mltB::tn* and (to a lesser degree) *sltY::tn* exhibited significantly increased survival in the presence of meropenem, with a drastic 1000-fold increase in survival after 24 hours for *mltB* and 100-fold for *sltY* (**Fig. 4A**). Time-dependent killing experiments confirmed a strong role for MltB as an antagonist of antibiotic tolerance, as the *mltB::tn* mutant exhibited minimal (5-fold) killing in the presence of meropenem over 24 hours (**Fig. 4B**).

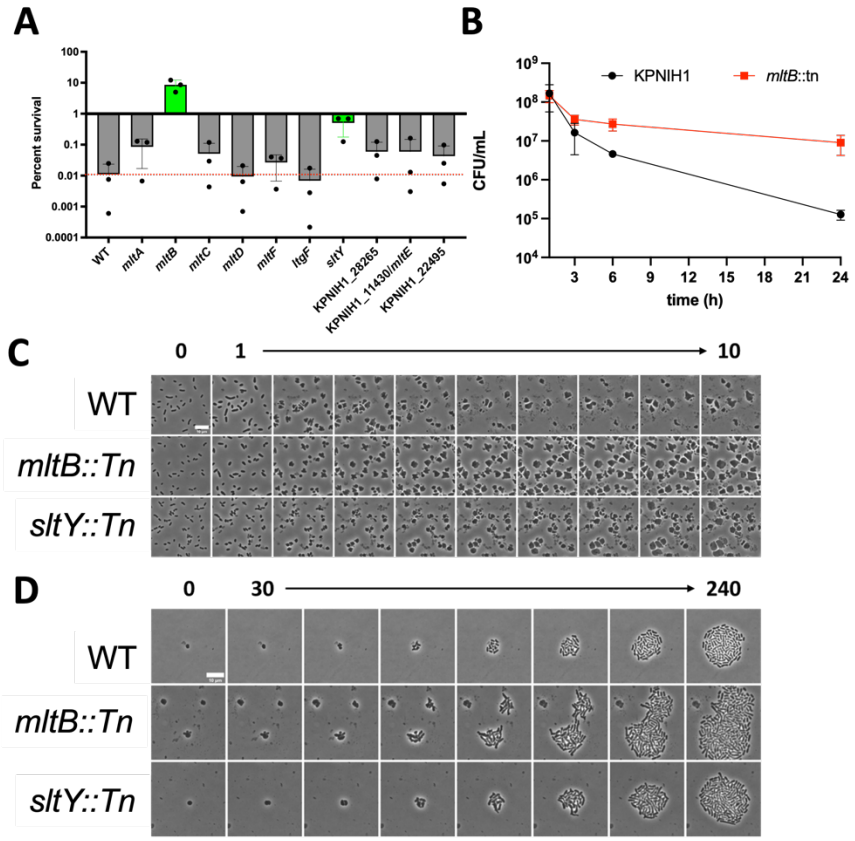

Figure 4: mltB and sltY reduce tolerance to meropenem and prevent cells from retaining polar morphology

(A) Survival of mutants in lytic transglycosylases. Mutants were obtained from the KPNIH1 mutant library and exposed to meropenem (10 µg/mL) for 6 hours, followed by dilution and spot-plating. (B) Time-dependent killing reveals increased tolerance in an *mltB* mutant. (C) Cell wall degradation in LTG mutants. Bacteria were applied to an

229 agarose pad containing BHI and 10 µg/mL meropenem. Images were taken every hour.
230 (D) Recovery dynamics of spheroplasts. Cells were treated with meropenem (10 µg/mL)
231 for 6 hours. Purified KPC-2 was then added, followed by timelapse microscopy.

232

233 The *mltB::tn* and *sltY:tn* mutants were further characterized by examining cell
234 morphology upon spheroplast formation and recovery. Timelapse microscopy of cells
235 exposed to meropenem revealed that the *mltB::tn* and *sltY:tn* disruption mutants retained
236 morphology at the cell poles for longer than the wild type parent strain, and qualitatively
237 exhibited an increase in the relative abundance of intact spheroplasts (**Fig. 4C**); this
238 coincided with qualitatively enhanced recovery dynamics (**Fig. 4D**). These data suggest
239 that *mltB* and (to a lesser extent) *sltY* reduce tolerance by accelerating the degradation
240 of peptidoglycan when synthesis is halted by meropenem, and thus point to a dominant
241 role of these LTGs in cell wall turnover in *K. pneumoniae*. These data suggest that
242 activation of autolysins could be a useful future strategy to potentiate β-lactam antibiotics
243 against tolerant pathogens.

244

245 *Multiple cell envelope stress responses systems collectively contribute to β-lactam*
246 *tolerance*

247 Several well-characterized cell envelope stress response systems appeared in our
248 screen as top candidates that promote meropenem tolerance: the Rcs phosphorelay
249 system, the PhoPQ and CpxAR two-component systems, and the osmotic and acid stress
250 response system, OmpR/EnvZ. Of note, our previous study revealed the PhoPQ system
251 as a key meropenem tolerance determinant in *Enterobacter cloacae,* suggesting that
252 PhoPQ may be a widely conserved tolerance determinant [25]. To dissect the individual

253 and combined contributions of these systems to survival in meropenem, we created
254 deletions of all four systems in all combinations, including one quadruple system deletion
255 mutant lacking all four stress responses. These mutants were then exposed to
256 meropenem in time-dependent killing assays. These experiments revealed a 10 to
257 10,000-fold decrease in viability after 24 hours of exposure to meropenem in any
258 individual envelope stress response mutant compared to the wild type *K. pneumoniae*
259 parent strain (**Fig. 5AB**). We observed large differences in both magnitude and
260 consequences for lysis in the different mutants. The Δ*ompR/envZ* mutant, for example,
261 exhibited the most drastic reduction in viability of all the single mutants (10,000-fold vs.
262 10- to 100-fold for the others), pointing to a particularly important role of the OmpR/EnvZ
263 response in tolerance to meropenem. We also noticed that while most single mutants
264 exhibited both a drop in cfu/mL and in OD_{600} (indicative of cell lysis), the Δ*rcsF* mutant
265 was only defective in viability, but increased in OD during meropenem treatment,
266 suggesting a role for Rcs in spheroplast recovery, rather than structural maintenance.

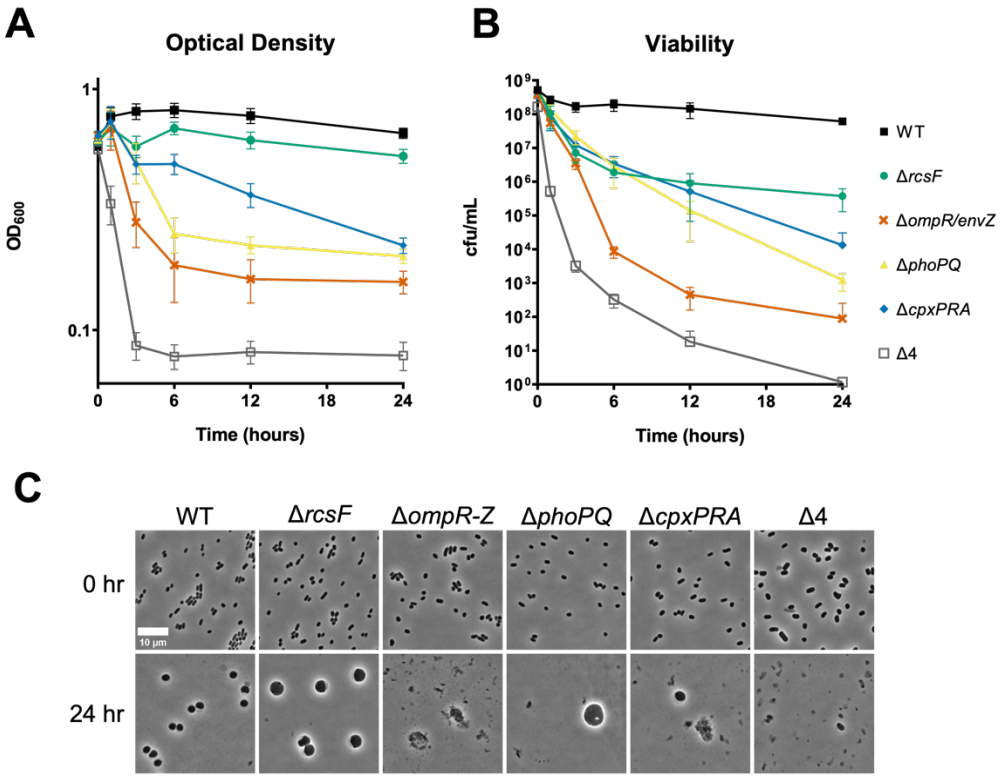

Figure 5: Cell envelope stress response systems are essential for full meropenem tolerance

Cells were diluted 10fold into 5 mL of BHI medium containing 10 µg/mL meropenem. At the indicated timepoints, samples were withdrawn and OD_{600} (A) and CFU/mL (B) were measured. (C) Aliquots were removed from the experiment depicted in (A-B) and imaged.

We also investigated cell morphologies of each mutant before and after exposure to meropenem for 24 hours of treatment, and upon recovery in strains capable of forming spheroplasts. Wild type cells and all single deletion mutants appeared similar in shape and morphology at the start of meropenem exposure experiments (**Fig. 5C**). However, the Δ4 mutant cells exhibited slightly aberrant morphology (slightly larger cells with subtle deformations) and spontaneous lysis, suggested by the presence of cell debris. After 24 hours of meropenem exposure, most single deletion mutants (with the exception of Δ*ompR/envZ*) formed spheroplasts with no clear difference in structure compared to the

282 wild type, albeit a much lower numbers (consistent with the decrease in OD_{600}).
283 Qualitatively, the microscopy analysis confirmed that the Rcs system does not appear to
284 be essential for structural maintenance of spheroplasts, as the Δ*rcsF* mutant showed little
285 evidence of lysis, and wild-type levels of spheroplasts (**Fig. 5C**). Thus, the Rcs system
286 may play a role in spheroplast recovery, rather than spheroplast cell envelope
287 maintenance, consistent with a role in spheroplast recovery in lysozyme-treated *E. coli*
288 [26]. Interestingly, the Δ*ompR/envZ* and Δ4 mutants were highly defective in spheroplast
289 formation or maintenance, as we failed to find any intact spheroplasts even upon 10-fold
290 concentration of meropenem-treated culture followed by imaging, consistent with the
291 drastic reduction in viability these strains experience in the presence of meropenem (**Fig.
292 5B**). We also constructed intermediate strains, including a suite of Δ3s with single two-
293 component systems left intact (**Fig. S3**). Interestingly, all Δ3s collapsed in viability almost
294 to the same degree as the Δ4, strongly suggesting an additive or synergistic effect
295 between the different systems, as no two-component system by itself could sustain
296 viability. Of note, among the Δ2 mutants, the combination of Δ*ompR/envZ* and Δ*rcs* was
297 most detrimental, and the resulting mutant was, like the Δ4 mutant, nearly eradicated after
298 24 hours of exposure. Collectively, these results point to a hierarchical organization of
299 responses necessary for meropenem tolerance; OmpR/EnvZ as the primary response,
300 followed by Pho and Cpx to maintain spheroplast stability, and Rcs to aid in recovery.

301

302 *The Rcs phosphorelay is induced by, and required for, meropenem tolerance*

303 The Rcs phosphorelay as an apparent contributor to tolerance caught our attention. In *E.
304 coli*, Rcs is induced by β-lactams, and required for survival in low β-lactam concentrations

305 [27]. Additionally, Rcs is required for recovery of *E. coli* from a cell wall-deficient state
306 (generated by lysozyme treatment in osmostabilized medium, a condition that
307 morphologically mimics meropenem-treated spheroplasts) [26]. In apparent contrast, a
308 recent study has shown that Rcs is neither induced by, nor required for β-lactam
309 persisters [28]; however, this is likely because persisters are dormant and thus not
310 expected to be damaged by the antibiotic (obviating the need for a damage response) [3].
311 To clarify the role of Rcs in *K. pneumoniae*, we engineered a TS1 strain carrying an P_{rprA}-
312 *lacZ* transcriptional fusion (a well-established readout of Rcs signaling [29]) in a neutral
313 chromosomal locus (*lacZ*) and measured induction by meropenem. A first qualitative
314 assay using zone of inhibition on growth medium containing the chromogenic LacZ
315 substrate X-gal yielded a blue ring around the zone of inhibition when a meropenem disk
316 was placed on the agar surface, but not when the translation inhibitor kanamycin was
317 used (**Fig. S4A**). We then corroborated these results in liquid medium, where a
318 quantitative β-galactosidase activity assay (Miller assay) revealed strong (30fold), time-
319 dependent induction of the construct by meropenem (**Fig. 6A**). Thus, meropenem induces
320 the Rcs response. We also validated the role of Rcs in meropenem tolerance by creating
321 additional mutants in Rcs components, namely RcsF, RcsC and RcsD. All mutants
322 displayed a strong (10,000fold) reduction in tolerance, which could be fully complemented
323 by overexpression of the response regulator RcsB (**Fig. 6B**). The ability of RcsB
324 overexpression to induce the Rcs regulon was verified by measuring induction of the
325 chromosomal P_{rprA}-*lacZ* construct (**Fig. S4B**). Thus, the Rcs phosphorelay is both
326 responsive to meropenem exposure, and required for meropenem tolerance in *K.*
327 *pneumoniae.*

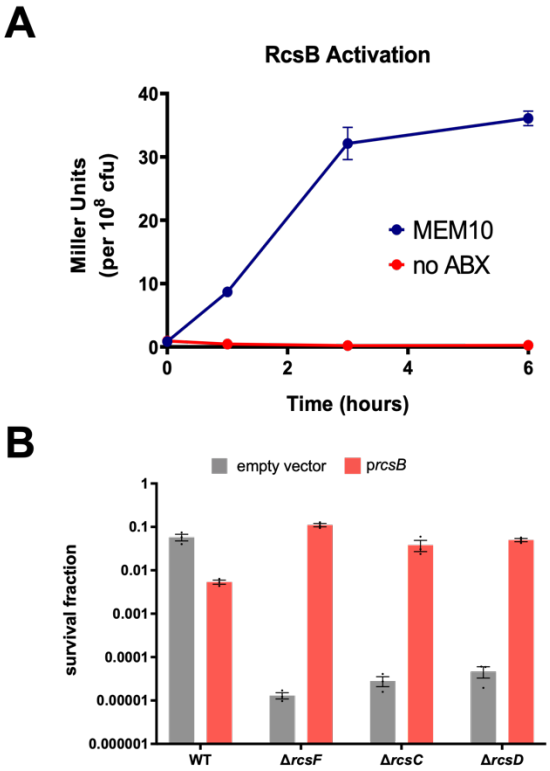

Figure 6: The Rcs phosphorelay is induced by meropenem and required for tolerance

(A) A strain carrying a chromosomal rprA-*lacZ* transcriptional fusion was exposed to meropenem, followed by quantification of beta-galactosidase activity via Miller assay (B) The indicated strains were exposed to meropenem (10 µg/mL). Survival fraction is CFU/mL after 24 hours normalized to starting cell density. Shown are averages of 3 independent experiments +/- standard error.

Fluctuation test reveals memory in tolerant subpopulation

The stress responses that contribute to meropenem tolerance may rely on deterministic induction by the antibiotic for their protective impact, or they may be stochastically and heterogeneously active within the population before exposure to a stress as a bet-hedging strategy. To gain some insight into this distinction, we leveraged the classical Luria-Delbrück experiment or the “Fluctuation Test” that has been recently expanded to

343 investigate reversible switching between cellular states within an isogenic cell population.
344 This fluctuation test has been used to gain insights into the non-genetic mechanisms by
345 which microbial and cancer cells survive lethal exposures to targeted drug therapy [30-
346 32]. For example, the application of the fluctuation test in both *Escherichia coli* [33] and
347 *Bacillus megaterium* [34] has shown individual cells to reversibly switch between an
348 antibiotic-sensitive and an antibiotic-tolerant state, with each state being maintained
349 transiently for several generations. This reversible switching happens continuously in the
350 absence of the drug as a result of stochastic fluctuations in underlying signaling and gene
351 regulatory networks and primes a rare subpopulation of cells as a bet-hedging
352 mechanism to survive lethal antibiotic exposure.

353 To conduct a fluctuation test, we first isolated single TS1 cells in 96-well plates
354 using serial dilution. Each cell was grown into a clonal population and exposed to
355 meropenem at an OD_{600} of 0.3 (**Fig. 7**). WT OD dropped sharply at first, followed by
356 slower increase in OD_{600} in the surviving subpopulation (spheroplasts). The clone-to-
357 clone fluctuations in cell viability after antibiotic exposure were quantified by using the
358 coefficient of variation (standard deviation divided by the mean) of OD_{600} (spheroplast
359 survivor fraction) across clones at 1.66 hours after drug exposure. This time point was
360 specifically chosen as it captures the OD_{600} drop-off in response to meropenem and
361 avoids the rebound in OD_{600} seen in WT cells as a result of changes in cell shape. We
362 then used mathematical modeling to predict how the kinetics of switching between drug-
363 sensitive and drug-tolerant cell states impact clone-to-clone fluctuations in the number of
364 cells surviving lethal stress, with slower switching (i.e., higher transient memory of a state
365 being retained across generation) resulting in a higher degree of interconal fluctuations

366 [32]. Our results show clone-to-clone fluctuations in cell integrity to be 0.153 ± 0.036 for
367 WT where ± denotes the 95% confidence intervals in the coefficient of variation of OD_{600}
368 as obtained by bootstrapping (**Fig. 7**). These observed fluctuations were significantly
369 higher than the technical noise of 0.086 ± 0.028 (control fluctuations). Technical noise
370 was estimated by performing a similar experiment, but with fluctuations quantified across
371 wells starting with a random population of 10,000 cells rather than a single cell-derived
372 population. Similar to observations in other bacteria, this fluctuation data is consistent
373 with a model of a multi-generation drug-tolerant state in *Klebsiella pneumoniae* that
374 preexists meropenem exposure.

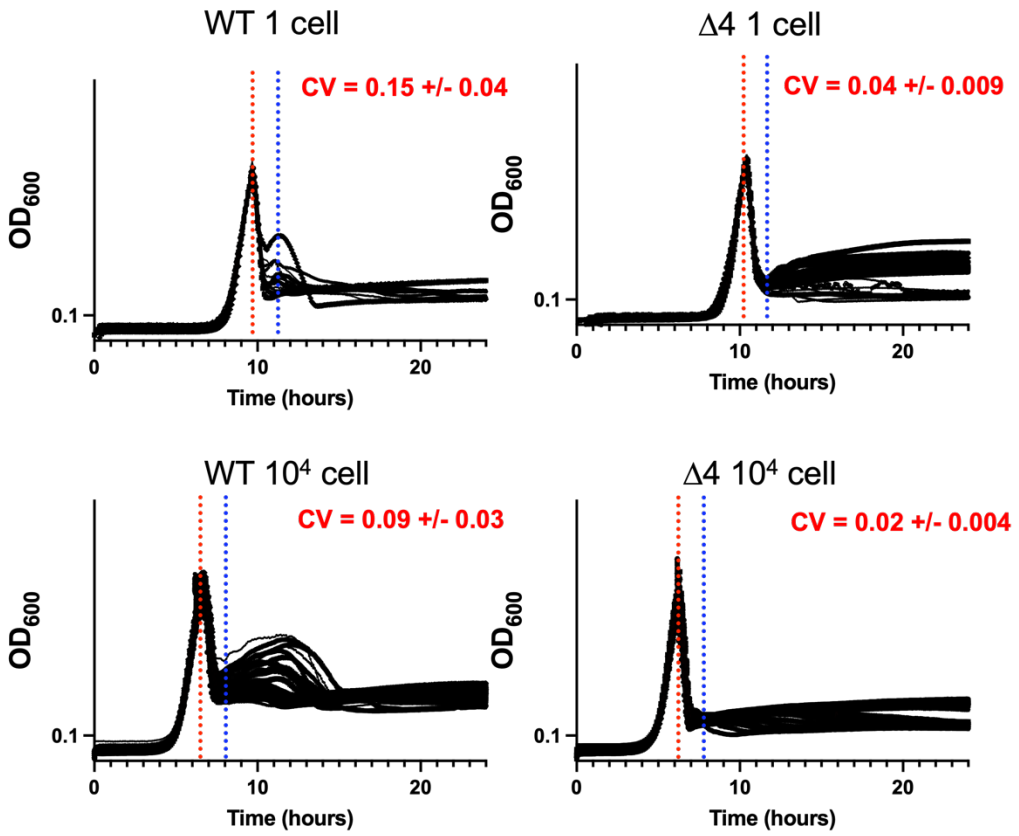

375

376 **Figure 7. Fluctuation test indicates memory in spheroplast population.** Bacteria
377 were diluted to a starting density of 1 cell/well or 10,000 cells/well (control), and grown
378 in a microtiter plate. At OD_{600} =0.3, meropenem (10 µg/mL) was added (red dotted line).

379 CV (coefficient of variation) calculations were performed at peak killing (blue dotted
380 line).

381

382 We hypothesized that the stochasticity originated from variance in background expression
383 of cell envelope stress responses. To test this, we repeated the fluctuation assay in the
384 Δ4 genotype where the observed fluctuations were interestingly much smaller compared
385 to WT with the coefficient of variation being 0.044±0.009, but still significant compared to
386 control fluctuations performed for this strain (**Fig. 7**). The lower value of the observed
387 clonal fluctuations in Δ4 points to faster-switching kinetics, and hence a shorter transient
388 memory of the drug-tolerant state.

389

390 **Discussion**

391 Infections with Enterobacterales continue to be an active and increasing threat to
392 public health due to their capacity to cause infection, and to gain and disseminate
393 antibiotic resistance genes, with particular risk for vulnerable populations. In this work, we
394 have found that antibiotic tolerance, the ability to sustain viability in the presence of
395 bactericidal antibiotics for extended time periods, is widespread among clinical isolates
396 of Gram-negative pathogens, particularly *Klebsiella pneumoniae*.

397 To uncover novel factors that modulate β-lactam tolerance in *K. pneumoniae* we
398 performed a genome-wide scan using a TnSeq approach. Because this approach
399 provides a readout of each gene's fitness during a challenge, we were able to identify
400 genes that contribute to meropenem tolerance, and genes that reduce tolerance in *K.*
401 *pneumoniae*. The screen overall was able to capture several regulatory systems and

402 individual factors that modulate tolerance along with the internal control PBP1b (a key
403 cell wall synthase required to rebuild the cell wall after catastrophic damage [23]), raising
404 confidence in our approach. This screen also pointed to several well-known and intensely
405 studied cell envelope stress responses that are partly responsible for this strain's ability
406 to undergo the entire process of spheroplast formation, maintenance, and recovery: the
407 Rcs, Pho, Cpx, and OmpR/EnvZ systems.

408 Interestingly, the OmpR/EnvZ system appears to exert an outsized effect on
409 tolerance. This system is induced by changes in pH and osmolarity, and controls the
410 switch from the larger diameter porin OmpF to the smaller diameter porin OmpC [35].
411 Formally, it is possible that the porin switch may delay diffusion of meropenem into the
412 cell; however, this is unlikely given that WT and Δ*ompR/envZ* MICs are within essential
413 agreement (**Table S2**). Future work will be directed at delineating the contribution of this
414 system to spheroplast maintenance. Conversely, the Pho and Cpx single system deletion
415 mutants appear to have similar net contributions to meropenem tolerance both in rate of
416 killing and final viability, while still forming detectable spheroplasts capable of recovery.
417 The versatile PhoPQ system senses Mg^{2+} deficiency, presence of antimicrobial peptides,
418 pH and other stresses [36]. Most relevant to the phenotype assayed here, we have
419 previously shown that PhoPQ is required for meropenem tolerance in the related
420 bacterium *Enterobacter cloacae*, via PhoPQ-controlled outer membrane modifications
421 [25]. The Cpx system is a general cell envelope health monitor [37], which controls,
422 among other things, L,D-transpeptidases that may help stabilize the outer membrane [38,
423 39], and respiratory chain functions [40, 41], which may contribute to ROS production in
424 spheroplasts [17]. Lastly, the Rcs system contributes to meropenem tolerance in a unique

425 way. Time-dependent killing revealed that viability dropped substantially in the Δ*rcsF*
426 mutant, but this strain's capacity to form spheroplasts and maintain optical density is
427 comparable to the WT parent strain. Interestingly, and consistent with previous work in *E.*
428 *coli* lysozyme-induced spheroplasts [26], Δ*rcsF* mutant spheroplasts were impaired in
429 their ability to reform successful dividing rods when meropenem is removed. Among other
430 genes, Rcs positively regulates the cell division component *ftsZ* [42], perhaps pointing to
431 a model where upon spheroplast recovery, cell division can commence sooner in WT
432 than in Δ*rcs* cells due to the increased availability of critical divisome components. Taken
433 together, the phenotypes of each individual mutant indicate that aspects of β-lactam
434 tolerance are mediated by distinct response systems, likely with some temporal distinction
435 (**Fig. 7**)

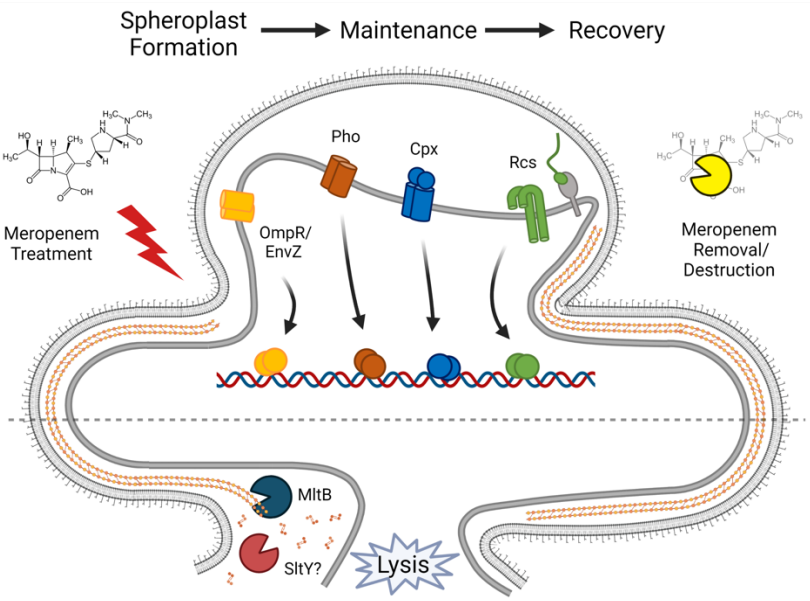

436

437

438 **Figure 8: Model of meropenem tolerance as a net result of cell wall degradation and**
439 **cell envelope stress response induction**

440 Meropenem treatment induces multiple cell envelope stress responses, whose regulons
441 contribute to survival. Lytic transglycosylases MltB and SltY contribute significantly to
442 sacculus degradation, which reduces efficiency of spheroplast recovery.

443

444 Because TnSeq has the benefit of also revealing gene disruptions that increase
445 fitness, we simultaneously probed for endogenous factors that reduce meropenem
446 tolerance. *K. pneumoniae* strain TS1's lytic transglycosylase *mltB* answered the screen
447 as a strong candidate that imparts a fitness increase when disrupted. Lytic
448 transglycosylases cleave glycosidic bonds of peptidoglycan strands [24], and have
449 specific and important functions in opportunistic pathogens. For example, in
450 *Acinetobacter baumannii*, *mltB* is a critical factor for pathogenesis by linking complex
451 envelope homeostasis functions with virulence [43]. In *Pseudomonas aeruginosa*,
452 eliminating this enzyme (also in combination with other lytic transglycosylases) increases
453 resistance to cell-wall targeting antibiotics via induction of an endogenous β-lactamase
454 [44, 45]. Disruption of *sltY* and *mltB* in *K. pneumoniae* strain KPNIH1 resulted in 10- 1000
455 fold increased tolerance to meropenem. Cell morphology around the poles in these
456 mutants was maintained after 24 hours of exposure to meropenem, possibly due to this
457 strain's inability to degrade the old peptidoglycan present when PBPs are inhibited. This
458 maintenance of the cell wall could be what increases survival by preserving the
459 peptidoglycan and envelope-spanning systems, leading to preservation of cell integrity
460 and potentially serving as a scaffold for new cell wall synthesis when meropenem is
461 removed. It is unclear why *mltB* and *sltY* specifically emerge as the only lytic
462 transglycosylases that have this effect on the cell when bacteria generally have multiple

463 redundant lytic transglycosylase paralogs in their genomes; strong phenotypes for single
464 deletion mutants are thus highly unusual.

465 This study presents a deeper insight into β-lactam tolerance and can inform further
466 investigations to understand other aspects of how these dangerous pathogens respond
467 to antibiotics and attain resistance. Attaining an understanding of the detailed workings
468 of this complex phenotype can inform approaches toward finding potential druggable
469 targets to reduce or abolish an organism's capacity for β-lactam tolerance, thus allowing
470 development of novel therapeutics and treatment strategies for tolerant pathogens.

471

472 **Methods**

473 *Culture conditions, tolerance measurement, and complementation*. Unless otherwise
474 stated, all strains were grown in shaking overnight cultures at 37ºC, and tolerance assays
475 were carried out in Brain Heart Infusion (BHI) broth at 37ºC. Tolerance assays were
476 conducted by inoculating overnight culture at a 1:10 ratio into fresh BHI medium
477 containing 10 µg/mL meropenem (TCI, Tokyo, Japan). Cultures were then incubated at
478 37˚C without shaking. Optical density was measured in a VWR V-1200
479 spectrophotometer and viable cells were quantified by serial dilution in BHI medium and
480 spot-titered onto BHI agar. The carbapenemase KPC-2 was purified and added to culture
481 samples at a final concentration of approximately 1 µg/mL prior to serial dilution to
482 deactivate meropenem, thus eliminating meropenem carryover effect.

483

484 *MIC Determination.* MICs for all strain backgrounds were determined by diluting overnight
485 cultures 10^7-fold in BHI medium. Diluted cultures were inoculated into BHI containing
486 successive 2-fold concentrations of meropenem in a 96 well microtiter plate at a final
487 volume of 200 µL per well, and incubated at 37°C overnight, leaving one well as an
488 uninoculated control, and one well with cells but without meropenem to ensure growth of
489 the strain. MICs were recorded as the lowest meropenem concentration free from
490 turbidity.

491

492 *Purification of* KPC-2 *enzyme*. The gene for KPC-2 was amplified from the genome of
493 *Enterobacter cloacae* strain 41952, a clinical isolate from WCM, and cloned into the
494 pET21 expression vector. The His-tagged KPC-2 enzyme was overexpressed in BL21
495 pLysS. A 500 ml culture of LB containing 100 µg/mL ampicillin was induced at OD=0.5
496 with 1 mM IPTG and incubated shaking at 30°C overnight. The following day, cultures
497 were centrifuged, and pellets were decanted and stored at -80°C until lysis and
498 purification. Pellets were resuspended in resuspension buffer (20 mM Tris, 150 mM NaCl,
499 5 mM imidazole) and sonicated using the QSonica with the largest tip attachment for 40
500 minutes total, alternating between 5 second pulses 5 second rests on ice. The lysate was
501 then centrifuged for 45 minutes at 16,000 rpm and the supernatant discarded. In
502 preliminary expression experiments, we found that KPC was mostly in the insoluble
503 fraction. The insoluble pellet was resuspended in binding buffer (20 mM Tris, 150 mM
504 NaCl, 5 mM imidazole, 3 M Urea), and incubated rotating overnight at 4°C to denature
505 and solubilize the KPC-2 protein. The next day, the denatured lysate was centrifuged
506 again at 16,000 rpm for 45 minutes, and the resulting supernatant passed through a

507 cobalt-charged NTA agarose resin column at room temperature. Six column volumes of
508 wash buffer (20 mM Tris, 150 mM NaCl, 30 mM imidazole, 3 M Urea) were then passed
509 through the column, and the protein eluted in 1.8 mL fractions with increasing
510 concentrations of imidazole in elution buffers (20 mM Tris, 150 mM NaCl, 50-600 mM
511 imidazole, 3 M Urea). Fractions with the highest protein concentrations were pooled, and
512 the total volume was dialyzed into a final storage buffer (20 mM Tris, 150 mM NaCl, 30%
513 glycerol) in three steps, each with decreasing concentrations of imidazole and increasing
514 concentrations of glycerol. Purity was determined by SDS-PAGE, and concentration was
515 estimated with Bio-Rad Bradford Assay kit.

516

517 *Imaging.* All images were taken on a Leica Mdi8 microscope (Leica Microsystems, GmbH,
518 Wetzlar, Germany) with a PECON TempController 2000-1 (Erbach, Germany), heated
519 stage at 37˚C for growth experiments, or room temperature for static images. For
520 timelapse microscopy of spheroplast formation, cells were placed on a 0.8% agarose pad
521 containing BHI and 10 µg/mL meropenem within a gene frame (ThermoFisher, Waltham,
522 MA). For recovery timelapses, KPC-2 enzyme was added at 5 µg/mL to eliminate the
523 meropenem. Frames were taken using autofocus control every five minutes for up to 12
524 hours. Timelapse video stacks were processed in FIJI (NIH) using the Linear Stack
525 Alignment with SIFT under the Registration plugin (using all default settings with the
526 exception of Expected Transformation, which was changed to Translation) to center cells
527 in the cropped frame. Frame rates were set at 3-4 frames per second for supplemental
528 videos.

529

530 *Transposon mutagenesis screen and data analysis*. *K. pneumoniae* strain TS1 was
531 mutagenized with a Mariner transposon delivered via the *E. coli* donor strain MFD λpir to
532 generate a complex library of kanamycin-resistant transposon mutants. This initial library
533 was frozen as a glycerol stock, and an overnight culture from it was grown in BHI
534 containing kanamycin at 50 µg/mL to form an input library as the comparison for TnSeq
535 analysis. Overnight cultures of this input library were diluted 10-fold into 5 mL BHI
536 containing meropenem (10 ug/mL) and incubated for six hours at 37˚C without shaking,
537 followed by plating on BHI agar plates after treatment with 5 µg/mLKPC-2 enzyme
538 (untreated controls were also generated mirroring the six-hour exposure and recovery
539 populations). Genomic DNA (gDNA) was extracted from all stages of the meropenem
540 challenge and recovery and prepared for Illumina sequencing. Briefly, gDNA extracted
541 from each library was sonicated to generate fragments mostly 200-800 base pairs long
542 which were blunted using NEB Quick Blunting Mix (#E1201L). After blunting, fragments
543 were given A-tails with Taq DNA polymerase to allow ligation of adapter sequences (full
544 lists of primers and reactions can be found in supplemental methods). Ligated fragments
545 were amplified with PCR to enrich transposon-adjacent regions, and then again were
546 PCR amplified with primers to add barcodes, spacer sequences, and Illumina chip
547 attachment ends. The library was run on agarose gel and all fragments 250-600 base
548 pairs were extracted for analysis on the BioAnylazer (Agilent, Santa Clara, CA) to assess
549 before Illumina sequencing. All libraries were sequenced as paired 150 bp reads, though
550 only forward reads were used in the final analysis.

551 Raw Illumina data were processed in Galaxy using the Cutadapt program to trim
552 reads for length and quality, then mapped with Bowtie2 using the *K. pneumoniae* TS1

553 FASTA reference genome available in NCBI (Biosample accession number
554 SAMN04014921) (full protocol available at this link:
555 https://usegalaxy.org/u/trevorcrossmicro/w/trimming). Mapped reads were analyzed by
556 TnSeq Explorer [46]to calculate insertion density of each gene from each library.
557 Insertion densities were used to calculate an insertion density ratio for each gene from
558 one library to another, thereby comparing essentiality across points in the meropenem
559 challenge. The comparison between library 2 (input) and library 6 (meropenem recovery)
560 was used as the basis for ranking genes in order of essentiality, with genes most essential
561 to meropenem tolerance appearing at the top of the list, while genes which impart a fitness
562 increase when disrupted appearing at the bottom of the list.

563

564 *KPNIH1 validations.* Candidate tolerance genes identified by TnSeq were first validated
565 using an arrayed *K. pneumoniae* KPNIH1 library constructed by the Manoil lab [21].
566 Transposon mutants were grown in 200 µL BHI medium overnight cultures in a 96 well
567 plate. The next day, the overnight culture was diluted 1:10 into BHI containing a final
568 concentration of 10 µg/mL meropenem. At the indicated time points, samples were taken
569 for cfu determination, while simultaneously measuring optical densities in a Spectramax
570 iX3 (Molecular Devices, San Jose, CA) plate reader, and then incubated at 37˚C without
571 shaking for six hours. Final optical density and cfu/mL were recorded and the ratio
572 between final and initial values were calculated to determine the effect of the gene
573 disruption when challenged with meropenem.

574

575 *Strain constructions with pTOX*. Strains and oligos are summarized in Table S3. Knock
576 out and reporter strains in *K. pneumoniae* TS1 were constructed using the pTOX5 allelic
577 exchange vector as described in [47]. Briefly, 800-1000 base pair regions flanking regions
578 were amplified using PCR or synthesized de novo and assembled via isothermal
579 assembly into the pTOX SmaI site. Assembled constructs were transformed into DH5α
580 λpir competent cells, plated on LB containing 100 µg/mL chloramphenicol and 1% glucose
581 (LB/CHL/gluc) (to repress the rhamnose inducible toxin gene) and screened for insertion
582 size with primers TC_82 and TC_83, followed by sequence verification through Sanger
583 sequencing. Correct constructs were transformed into conjugal MFD λpir and mated into
584 *K. pneumoniae* TS1 on LB containing 1% glucose and 1.2 mM DAP (LB/gluc/DAP) for 6
585 hours at 37°C. Transconjugants were isolated back on LB/CHL/gluc and a single colony
586 was grown out in LB containing 1% glucose until the OD reached 0.1-0.2, at which point
587 cells were washed with M9 medium containing 0.2% casamino acids and 1% rhamnose,
588 and plated on solid M9/rham/casamino acids to induce the counterselective toxin and
589 isolate allelic exchange constructs containing the desired modifications. Envelope stress
590 response system deletions were screened using primers flanking the loci of interest and
591 validated using internal primers. Other constructs were validated using primers specific
592 to the modification, or primers flanking the *lac*/Z locus where reporters were inserted.

593

594 *Miller assay to detect RcsB function and induction*. To assess function of the RcsB
595 response regulator, a reporter construct was made by inserting an *rprA-lacZ*$_{MG1655}$
596 reporter with the *E. coli* MG1655 lacZ gene (abbreviated to *rprA-lacZ*) into the TS1 native
597 *lacZ* locus, eliminating most of the native *lacI* and *lacZ* genes. This construct was

598 validated first by overexpressing native RcsB on a pBAD plasmid in the presence of 0.2%
599 arabinose on BHI medium from strain TS1 in the reporter background and qualitatively
600 comparing X-gal signal to the construct containing an empty vector. RcsB activation upon
601 meropenem exposure was measured by performing the Miller assay on cell pellets from
602 meropenem-exposed cells at 0, 1, 3, and 6 hours in BHI and control cultures to determine
603 relative units of β-galactosidase activity normalized to cfu/mL of either culture.

604

605 **Acknowledgements**

606 This work was supported by NIH-NIAID grant R01AI143704 to TD.
607 AS acknowledges support from NIH-NIGMS via grant R35GM148351.

608

609

610

611

612

613

614

615

616

617

618 **Supplementary Figures**

619

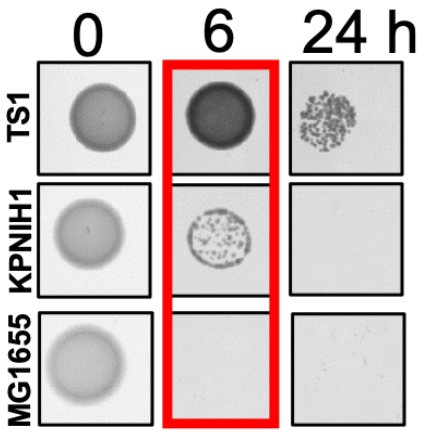

620

621 **Fig. S1 Tolerance screen validation with benchmark isolates**

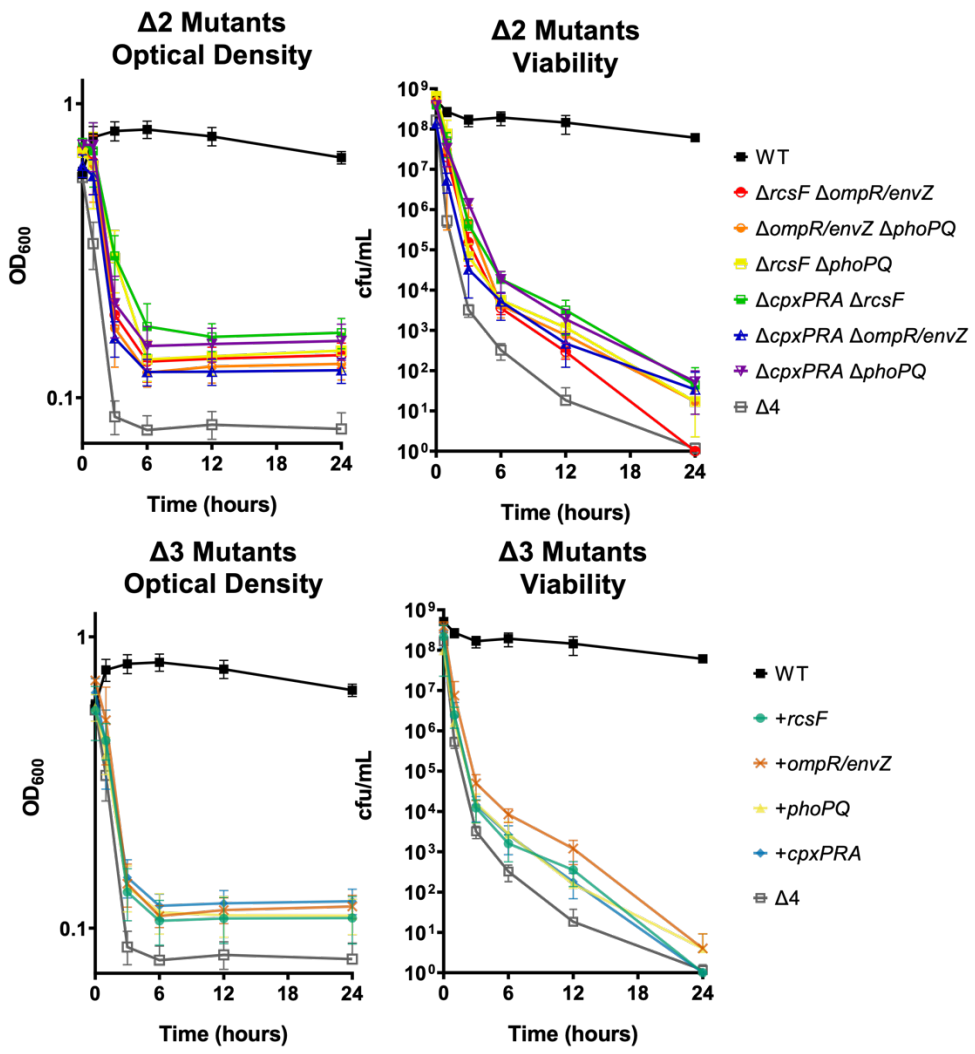

Fig. S2 Tolerance phenotypes of CESR mutants

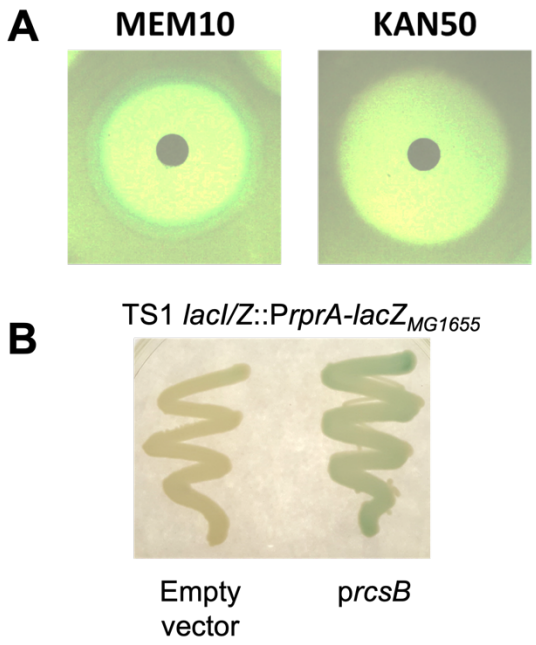

624

625 **Fig. S3 Meropenem induces the Rcs phosphorelay**

626

627 **Supplementary Tables** (preprint version: available upon request

628 tdoerr@cornell.edu)

629 Table S1 – Bloodstream isolate panel with MIC data

Strain	**MIC (µg/mL)** **(n=3 replicates)**
TS1 WT	0.00625
TS1 Δ*rcsF*	0.00625

TS1 Δ*ompR/envZ*	0.003125
TS1 Δ*phoPQ*	0.00625
TS1 Δ*cpxPRA*	0.003125
TS1 Δ*4*	0.001563
KPNIH1 WT	0.05
KPNIH1 *mltB::tn*	0.8
KPNIH1 *sltY::tn*	0.2
MG1655 WT	0.003125

630

631 Table S2 – MICs of strains constructed in this study

632 Table S3 – Strains and Oligos

633 Table S4 – TnSeq hits raw data

634

635

636

637

638 ## References:

639 1. Miller WR, Arias CA. ESKAPE pathogens: antimicrobial resistance, epidemiology, clinical
640 impact and therapeutics. Nat Rev Microbiol. 2024;22(10):598-616. Epub 2024/06/04. doi:
641 10.1038/s41579-024-01054-w. PubMed PMID: 38831030.
642 2. Haney EF, Hancock REW. Addressing Antibiotic Failure—Beyond Genetically Encoded
643 Antimicrobial Resistance. Frontiers in Drug Discovery. 2022;2. doi: 10.3389/fddsv.2022.892975.
644 3. Balaban NQ, Helaine S, Lewis K, Ackermann M, Aldridge B, Andersson DI, et al.
645 Definitions and guidelines for research on antibiotic persistence. Nat Rev Microbiol.
646 2019;17(7):441-8. Epub 2019/04/14. doi: 10.1038/s41579-019-0196-3. PubMed PMID:
647 30980069; PubMed Central PMCID: PMCPMC7136161.
648 4. Roberts D, Higgs E, Rutman a, Cole P. Isolation of spheroplastic forms of Haemophilus
649 influenzae from sputum in conventionally treated chronic bronchial sepsis using selective medium
650 supplemented with N-acetyl-D-glucosamine: possible reservoir for re-emergence of infection.
651 British medical journal (Clinical research ed). 1984;289:1409-12. doi:
652 10.1016/j.compmedimag.2005.07.001. PubMed PMID: 6437576.
653 5. Monahan LG, Turnbull L, Osvath SR, Birch D, Charles IG, Whitchurch CB. Rapid
654 conversion of Pseudomonas aeruginosa to a spherical cell morphotype facilitates tolerance to
655 carbapenems and penicillins but increases susceptibility to antimicrobial peptides. Antimicrob
656 Agents Chemother. 2014;58(4):1956-62. doi: 10.1128/AAC.01901-13. PubMed PMID: 24419348;
657 PubMed Central PMCID: PMCPMC4023726.
658 6. Dörr T, Davis BM, Waldor MK. Endopeptidase-mediated beta lactam tolerance. PLoS
659 Pathog. 2015;11(4):e1004850. doi: 10.1371/journal.ppat.1004850. PubMed PMID: 25884840;
660 PubMed Central PMCID: PMCPMC4401780.
661 7. Cross T, Ransegnola B, Shin JH, Weaver A, Fauntleroy K, VanNieuwenhze MS, et al.
662 Spheroplast-Mediated Carbapenem Tolerance in Gram-Negative Pathogens. Antimicrob Agents
663 Chemother. 2019;63(9). doi: 10.1128/AAC.00756-19. PubMed PMID: 31285232; PubMed Central
664 PMCID: PMCPMC6709500.
665 8. Mickiewicz KM, Kawai Y, Drage L, Gomes MC, Davison F, Pickard R, et al. Possible role
666 of L-form switching in recurrent urinary tract infection. Nat Commun. 2019;10(1):4379. Epub
667 2019/09/29. doi: 10.1038/s41467-019-12359-3. PubMed PMID: 31558767; PubMed Central
668 PMCID: PMCPMC6763468.
669 9. Claessen D, Errington J. Cell Wall Deficiency as a Coping Strategy for Stress. Trends
670 Microbiol. 2019;27(12):1025-33. Epub 2019/08/20. doi: 10.1016/j.tim.2019.07.008. PubMed
671 PMID: 31420127.
672 10. Errington J. Cell wall-deficient, L-form bacteria in the 21st century: a personal perspective.
673 Biochemical Society Transactions. 2017;45:287-95. doi: 10.1042/BST20160435. PubMed PMID:
674 28408469.
675 11. Paczosa MK, Mecsas J. Klebsiella pneumoniae: Going on the Offense with a Strong
676 Defense. Microbiol Mol Biol Rev. 2016;80(3):629-61. Epub 2016/06/17. doi:
677 10.1128/mmbr.00078-15. PubMed PMID: 27307579; PubMed Central PMCID:
678 PMCPMC4981674.
679 12. Murray CJL, Ikuta KS, Sharara F, Swetschinski L, Robles Aguilar G, Gray A, et al. Global
680 burden of bacterial antimicrobial resistance in 2019: a systematic analysis. The Lancet.
681 2022;399(10325):629-55. doi: 10.1016/S0140-6736(21)02724-0.
682 13. Chen TA, Chuang YT, Lin CH. A Decade-Long Review of the Virulence, Resistance, and
683 Epidemiological Risks of Klebsiella pneumoniae in ICUs. Microorganisms. 2024;12(12). Epub
684 2025/01/08. doi: 10.3390/microorganisms12122548. PubMed PMID: 39770751; PubMed Central
685 PMCID: PMCPMC11678397.

686 14. Dörr T. Understanding tolerance to cell wall–active antibiotics. Annals of the New York
687 Academy of Sciences. 2021;1496(1):35-58. doi: https://doi.org/10.1111/nyas.14541.
688 15. Cho H, Uehara T, Bernhardt TG. Beta-lactam antibiotics induce a lethal malfunctioning of
689 the bacterial cell wall synthesis machinery. Cell. 2014;159(6):1300-11. doi:
690 10.1016/j.cell.2014.11.017. PubMed PMID: 25480295; PubMed Central PMCID:
691 PMCPMC4258230.
692 16. Lobritz MA, Andrews IW, Braff D, Porter CBM, Gutierrez A, Furuta Y, et al. Increased
693 energy demand from anabolic-catabolic processes drives β-lactam antibiotic lethality. Cell Chem
694 Biol. 2022;29(2):276-86.e4. Epub 2022/01/07. doi: 10.1016/j.chembiol.2021.12.010. PubMed
695 PMID: 34990601; PubMed Central PMCID: PMCPMC8857051.
696 17. Shin JH, Choe D, Ransegnola B, Hong HR, Onyekwere I, Cross T, et al. A multifaceted
697 cellular damage repair and prevention pathway promotes high-level tolerance to beta-lactam
698 antibiotics. EMBO Rep. 2021:e51790. Epub 2021/01/20. doi: 10.15252/embr.202051790.
699 PubMed PMID: 33463026.
700 18. Held K, Gasper J, Morgan S, Siehnel R, Singh P, Manoil C. Determinants of Extreme beta-
701 Lactam Tolerance in the Burkholderia pseudomallei Complex. Antimicrob Agents Chemother.
702 2018;62(4). doi: 10.1128/AAC.00068-18. PubMed PMID: 29439964; PubMed Central PMCID:
703 PMCPMC5913950.
704 19. Dörr T, Alvarez L, Delgado F, Davis BM, Cava F, Waldor MK. A cell wall damage response
705 mediated by a sensor kinase/response regulator pair enables beta-lactam tolerance. Proc Natl
706 Acad Sci U S A. 2016;113(2):404-9. doi: 10.1073/pnas.1520333113. PubMed PMID: 26712007;
707 PubMed Central PMCID: PMCPMC4720315.
708 20. Gefen O, Chekol B, Strahilevitz J, Balaban NQ. TDtest: easy detection of bacterial
709 tolerance and persistence in clinical isolates by a modified disk-diffusion assay. Sci Rep.
710 2017;7:41284. doi: 10.1038/srep41284. PubMed PMID: 28145464; PubMed Central PMCID:
711 PMCPMC5286521 financial interests in this work.
712 21. Ramage B, Erolin R, Held K, Gasper J, Weiss E, Brittnacher M, et al. Comprehensive
713 Arrayed Transposon Mutant Library of Klebsiella pneumoniae Outbreak Strain KPNIH1. J
714 Bacteriol. 2017;199(20). doi: 10.1128/JB.00352-17. PubMed PMID: 28760848; PubMed Central
715 PMCID: PMCPMC5637181.
716 22. Weaver AI, Murphy SG, Umans B, Tallavajhala S, Onyekwere I, Wittels S, et al. Genetic
717 determinants of penicillin tolerance in Vibrio cholerae. Antimicrob Agents Chemother. 2018. doi:
718 10.1128/AAC.01326-18. PubMed PMID: 30061291.
719 23. Ranjit DK, Jorgenson MA, Young KD. PBP1B Glycosyltransferase and Transpeptidase
720 Activities Play Different Essential Roles during the De Novo Regeneration of Rod Morphology in
721 Escherichia coli. J Bacteriol. 2017;199(7). Epub 2017/01/18. doi: 10.1128/jb.00612-16. PubMed
722 PMID: 28096447; PubMed Central PMCID: PMCPMC5350282.
723 24. Weaver A, Taguchi A, Dörr T. Masters of Misdirection: Peptidoglycan Glycosidases in
724 Bacterial Growth. J Bacteriol. 2023;205(3):e0042822. Epub 2023/02/10. doi: 10.1128/jb.00428-
725 22. PubMed PMID: 36757204; PubMed Central PMCID: PMCPMC10029718.
726 25. Murtha AN, Kazi MI, Schargel RD, Cross T, Fihn C, Cattoir V, et al. High-level carbapenem
727 tolerance requires antibiotic-induced outer membrane modifications. PLoS Pathog.
728 2022;18(2):e1010307. Epub 20220207. doi: 10.1371/journal.ppat.1010307. PubMed PMID:
729 35130322; PubMed Central PMCID: PMCPMC8853513.
730 26. Ranjit DK, Young KD. The Rcs stress response and accessory envelope proteins are
731 required for de novo generation of cell shape in Escherichia coli. J Bacteriol. 2013;195(11):2452-
732 62. Epub 2013/04/02. doi: 10.1128/JB.00160-13. PubMed PMID: 23543719; PubMed Central
733 PMCID: PMCPMC3676047.
734 27. Laubacher ME, Ades SE. The Rcs phosphorelay is a cell envelope stress response
735 activated by peptidoglycan stress and contributes to intrinsic antibiotic resistance. J Bacteriol.

2008;190(6):2065-74. doi: 10.1128/JB.01740-07. PubMed PMID: 18192383; PubMed Central PMCID: PMCPMC2258881.
28. Rousseau CJ, Fraikin N, Zedek S, Van Melderen L. Are envelope stress responses essential for persistence to β-lactams in Escherichia coli? Antimicrob Agents Chemother. 2023;67(10):e0032923. Epub 2023/10/03. doi: 10.1128/aac.00329-23. PubMed PMID: 37787525; PubMed Central PMCID: PMCPMC10583663.
29. Wall E, Majdalani N, Gottesman S. The Complex Rcs Regulatory Cascade. Annu Rev Microbiol. 2018;72:111-39. doi: 10.1146/annurev-micro-090817-062640. PubMed PMID: 29897834.
30. Harmange G, Hueros RAR, Schaff DL, Emert B, Saint-Antoine M, Kim LC, et al. Disrupting cellular memory to overcome drug resistance. Nature Communications. 2023;14(1):7130. doi: 10.1038/s41467-023-41811-8.
31. Shaffer SM, Dunagin MC, Torborg SR, Torre EA, Emert B, Krepler C, et al. Rare cell variability and drug-induced reprogramming as a mode of cancer drug resistance. Nature. 2017;546(7658):431-5. doi: 10.1038/nature22794.
32. Singh A, Saint-Antoine M. Probing transient memory of cellular states using single-cell lineages. Frontiers in Microbiology. 2023;13. doi: 10.3389/fmicb.2022.1050516.
33. Hossain T, Singh A, Butzin NC. Escherichia coli cells are primed for survival before lethal antibiotic stress. Microbiology Spectrum. 2023;11(5):e01219-23. doi: doi:10.1128/spectrum.01219-23.
34. Guha M, Singh A, Butzin NC. Gram-positive bacteria are primed for surviving lethal doses of antibiotics and chemical stress. bioRxiv. 2024:2024.05.28.596288. doi: 10.1101/2024.05.28.596288.
35. Kenney LJ, Anand GS. EnvZ/OmpR Two-Component Signaling: An Archetype System That Can Function Noncanonically. EcoSal Plus. 2020;9(1). Epub 2020/02/01. doi: 10.1128/ecosalplus.ESP-0001-2019. PubMed PMID: 32003321; PubMed Central PMCID: PMCPMC7192543.
36. Groisman EA, Duprey A, Choi J. How the PhoP/PhoQ System Controls Virulence and Mg(2+) Homeostasis: Lessons in Signal Transduction, Pathogenesis, Physiology, and Evolution. Microbiol Mol Biol Rev. 2021;85(3):e0017620. Epub 2021/07/01. doi: 10.1128/mmbr.00176-20. PubMed PMID: 34191587; PubMed Central PMCID: PMCPMC8483708.
37. Raivio TL. Everything old is new again: an update on current research on the Cpx envelope stress response. Biochim Biophys Acta. 2014;1843(8):1529-41. Epub 2013/11/05. doi: 10.1016/j.bbamcr.2013.10.018. PubMed PMID: 24184210.
38. Morè N, Martorana AM, Biboy J, Otten C, Winkle M, Serrano CKG, et al. Peptidoglycan Remodeling Enables Escherichia coli To Survive Severe Outer Membrane Assembly Defect. mBio. 2019;10(1). Epub 2019/02/07. doi: 10.1128/mBio.02729-18. PubMed PMID: 30723128; PubMed Central PMCID: PMCPMC6428754.
39. Bernal-Cabas M, Ayala JA, Raivio TL. The Cpx envelope stress response modifies peptidoglycan cross-linking via the L,D-transpeptidase LdtD and the novel protein YgaU. J Bacteriol. 2015;197(3):603-14. Epub 2014/11/26. doi: 10.1128/jb.02449-14. PubMed PMID: 25422305; PubMed Central PMCID: PMCPMC4285979.
40. Guest RL, Wang J, Wong JL, Raivio TL. A Bacterial Stress Response Regulates Respiratory Protein Complexes To Control Envelope Stress Adaptation. J Bacteriol. 2017;199(20). Epub 2017/08/02. doi: 10.1128/jb.00153-17. PubMed PMID: 28760851; PubMed Central PMCID: PMCPMC5637174.
41. Tsviklist V, Guest RL, Raivio TL. The Cpx Stress Response Regulates Turnover of Respiratory Chain Proteins at the Inner Membrane of Escherichia coli. Front Microbiol. 2021;12:732288. Epub 2022/02/15. doi: 10.3389/fmicb.2021.732288. PubMed PMID: 35154019; PubMed Central PMCID: PMCPMC8831704.

42. Carballès F, Bertrand C, Bouché JP, Cam K. Regulation of Escherichia coli cell division genes ftsA and ftsZ by the two-component system rcsC-rcsB. Mol Microbiol. 1999;34(3):442-50. Epub 1999/11/17. doi: 10.1046/j.1365-2958.1999.01605.x. PubMed PMID: 10564486.
43. Crépin S, Ottosen EN, Peters K, Smith SN, Himpsl SD, Vollmer W, et al. The lytic transglycosylase MltB connects membrane homeostasis and in vivo fitness of Acinetobacter baumannii. Mol Microbiol. 2018;109(6):745-62. Epub 2018/06/10. doi: 10.1111/mmi.14000. PubMed PMID: 29884996; PubMed Central PMCID: PMCPMC6185781.
44. Cavallari JF, Lamers RP, Scheurwater EM, Matos AL, Burrows LL. Changes to its peptidoglycan-remodeling enzyme repertoire modulate β-lactam resistance in Pseudomonas aeruginosa. Antimicrob Agents Chemother. 2013;57(7):3078-84. Epub 2013/04/25. doi: 10.1128/aac.00268-13. PubMed PMID: 23612194; PubMed Central PMCID: PMCPMC3697359.
45. Lamers RP, Nguyen UT, Nguyen Y, Buensuceso RN, Burrows LL. Loss of membrane-bound lytic transglycosylases increases outer membrane permeability and β-lactam sensitivity in Pseudomonas aeruginosa. Microbiologyopen. 2015;4(6):879-95. Epub 2015/09/17. doi: 10.1002/mbo3.286. PubMed PMID: 26374494; PubMed Central PMCID: PMCPMC4694138.
46. Solaimanpour S, Sarmiento F, Mrázek J. Tn-Seq Explorer: A Tool for Analysis of High-Throughput Sequencing Data of Transposon Mutant Libraries. PLOS ONE. 2015;10(5):e0126070. doi: 10.1371/journal.pone.0126070.
47. Lazarus JE, Warr AR, Kuehl CJ, Giorgio RT, Davis BM, Waldor MK. A New Suite of Allelic-Exchange Vectors for the Scarless Modification of Proteobacterial Genomes. Appl Environ Microbiol. 2019;85(16). Epub 2019/06/16. doi: 10.1128/aem.00990-19. PubMed PMID: 31201277; PubMed Central PMCID: PMCPMC6677854.